Electronic Supplementary Material (ESI) for Nanoscale.

Supporting information for

Interfacial Engineering of Ni-Co-Mn@Ni Nanosheets-Nanocones Arrays for High performance Non-Noble Metal Electrocatalyst for Hydrogen Generation.

Mostafa Nazemi[a], Ghasem Barati Darband[a]*, Ali Davoodi[b]

a- Materials and Metallurgical Engineering Department, Faculty of Engineering, Ferdowsi University of Mashhad, Mashhad 91775-1111, Iran

b- Amsterdam science park, PC1098X, Netherlands

Corresponding author: (Ghasem Barati Darband: baratidarband@um.ac.ir)

Table S1. Chemical composition of electrodeposition baths

Component	NNCs Bath (mol.lit^{-1})	NCMNSs Bath (mol.lit^{-1})
$NiCl_2.6H_2O$	1	0.01
NH_3	2	-
NH_4Cl	3	-
$CoCl_2.6H_2O$	-	0.01
$MnCl_2.4H_2O$	-	0.01

Table S2. Cyclic electrodeposition parameters and samples names

Sample Name	number of cycles	scan rate (mV.s^{-1})
1C-S10	1	10
3C-S10	3	10
5C-S10	5	10
10C-S10	10	10
3C-S20	3	20
3C-S50	3	50
3C-S80	3	80

Table S3. C_{dl} and ECSA extracted from CV curves

Parameter	C1	C3	C5	C10	S20	S50	S80	NiCo
C_{dl} ($mF.cm^{-2}$)	55.3	60.9	57	41.9	59.8	3.1	0.7	58.2
ECSA (cm^2)	2765	3045	2850	2095	2990	155	35	2910

Table S4. Tafel slope for each step of HER

Step	Tafel Slope ($mV.dec^{-1}$)
Volmer	120
Heyrovsky	40
Tafel	30

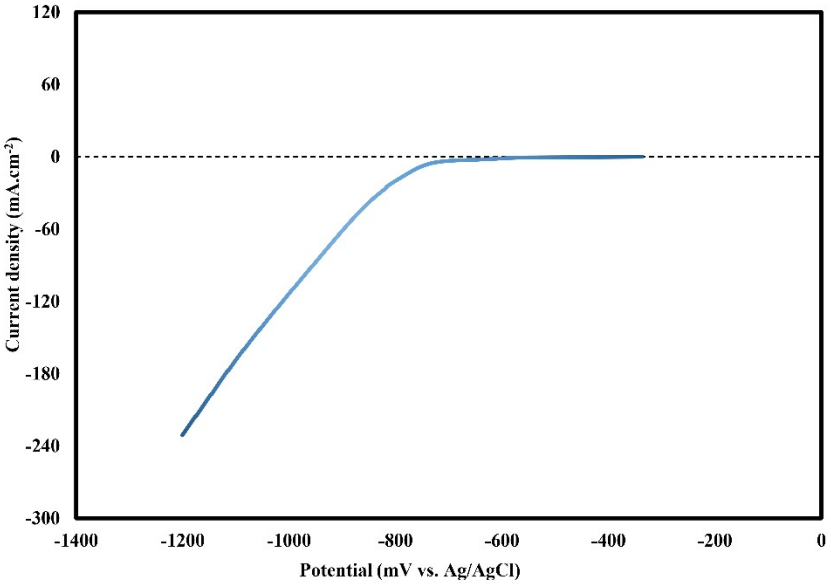

Figure S1. LSV curve of NF in first deposition bath

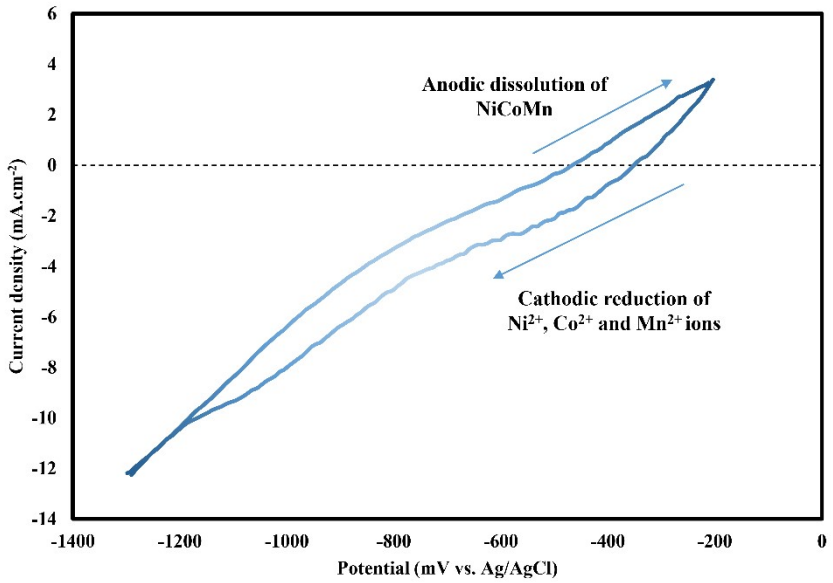

Figure S2. Cyclic voltammetry electrodeposition of NiCoMn nanosheets at 50 mV.s^{-1} sweep rate

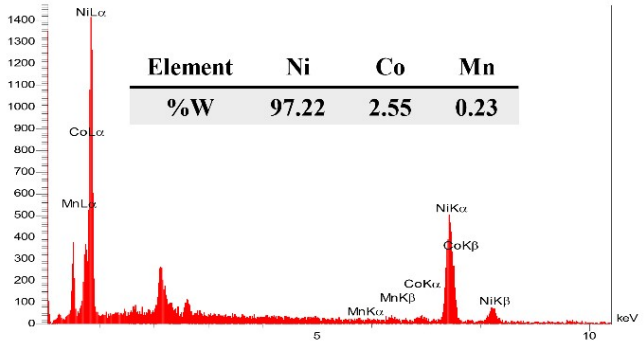

Element	Ni	Co	Mn
%W	97.22	2.55	0.23

Figure S3. EDX results and corresponding weight percentages of C3-S80

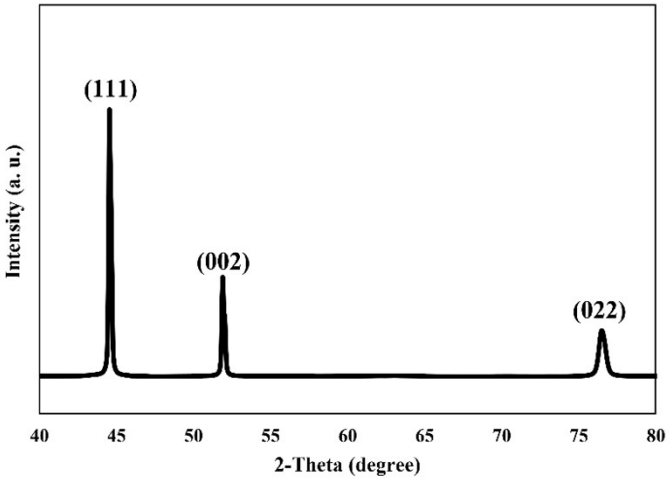

Figure S4. XRD pattern of C3-S10 sample ((Reference code: 96-432-0487)

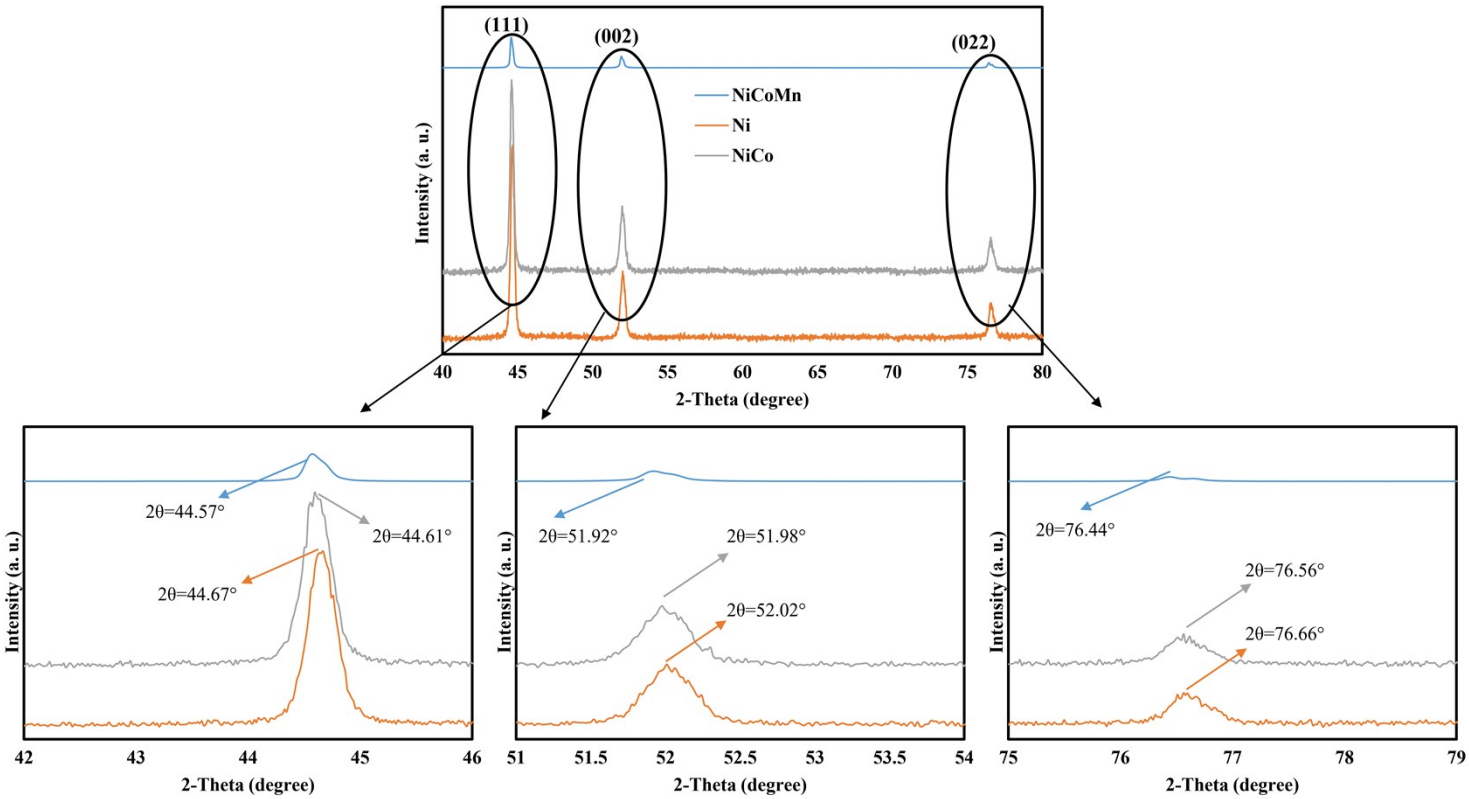

Figure S5; XRD patterns of different stages: NNCs, NiCo and NiCoMn (Reference code: 96-432-0487)

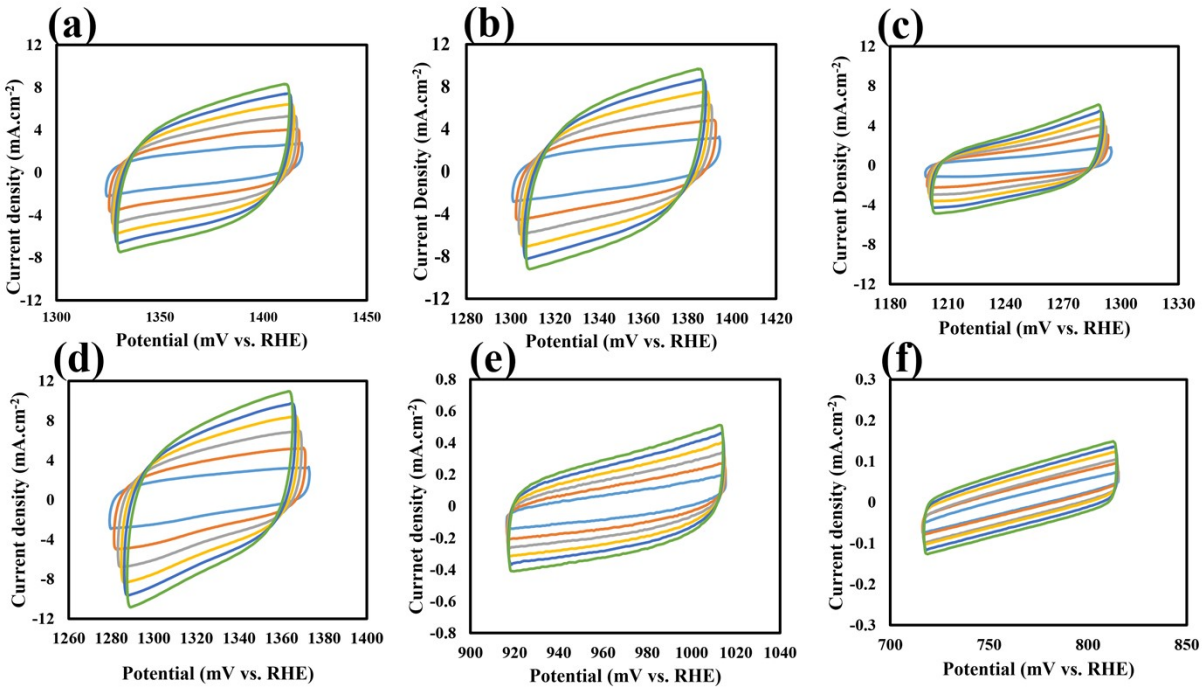

Figure S6. CV curves in different sweep rates for ECSA measurements of a) C1-S10 b) C5-S10 c) C10-S10 d) C3-S20 e) C3-S50 and f) C3-S80, respectively

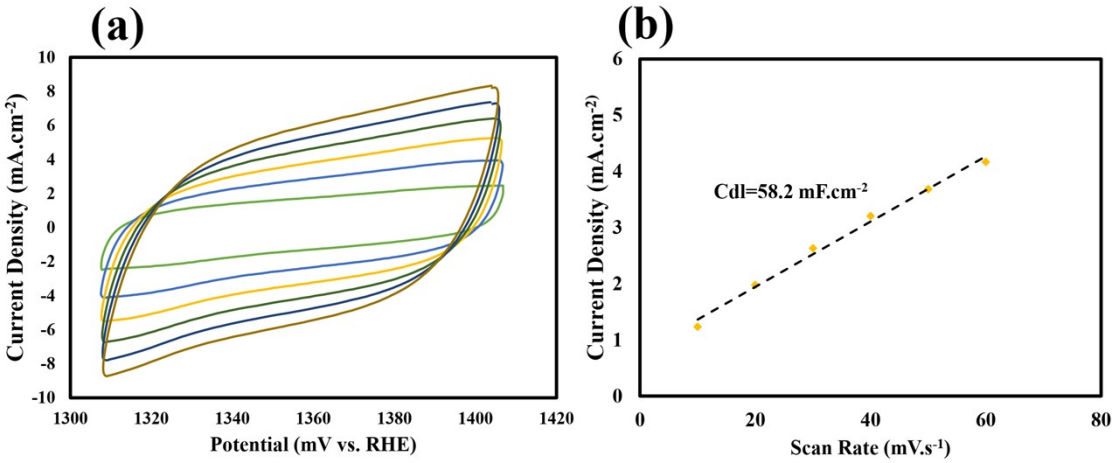

Figure S7. a) CV curves in different sweep rates for ECSA measurement and b) linear plot for Cdl extraction of NiCo sample

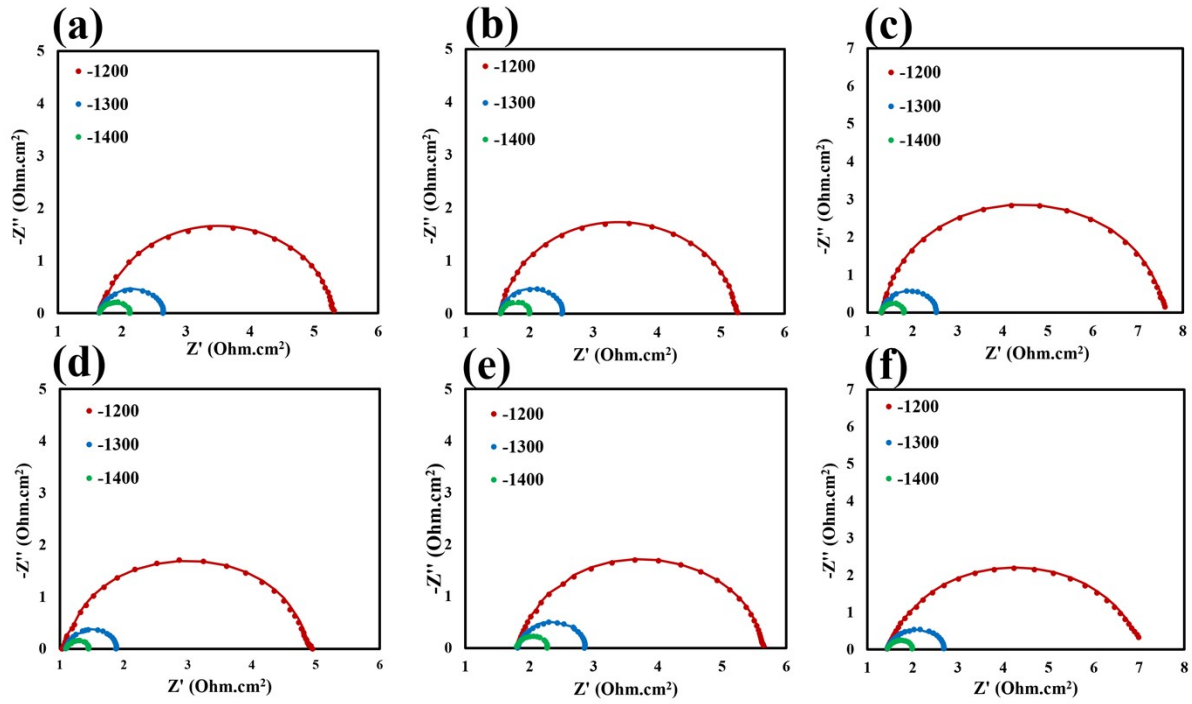

Figure S8. Nyquist plots of a) C1-S10, b) C5-S10, c) C10-S10, d) C3-S20, e) C3-S50 and f) NNCs substrate, respectively

TableS5. Electrochemical parameters determined from Nyquist plots

	-1200				-1300				-1400			
Sample	**R_s**	**CPE**	**n**	**R_{CT}**	**R_s**	**CPE**	**n**	**R_{CT}**	**R_s**	**CPE**	**n**	**R_{CT}**
NNCs	1.431	5.419m	843.007m	5.666	1.429	2.968m	894.5m	1.266	1.442	1.82m	946m	570.879m
C1-S10	1.723	4.661m	954.575m	3.563	1.667	3.144m	975.287m	974.774m	1.645	10.286m	791.903m	501.881m
C3-S10	1.263	9.962m	979.51m	3.53	1.265	6.285m	990.15m	840.605m	1.238	9.024m	895.979m	429.561m
C5-S10	1.572	7.069m	966.408m	3.652	1.546	4.566m	980.999m	972.369m	1.539	10.093m	839.755m	485.957m
C10-S10	1.334	6.711m	944.942m	6.251	1.313	4.053m	976.57m	1.212	1.302	3.191m	975.263m	505.946m
C3-S20	1.065	7.608m	922.407m	3.845	1.089	4.1m	973.541m	840.8m	1.1	2.997m	979.976m	353.092m
C3-S50	1.81	3.085m	927.537m	3.85	1.836	1.628m	993m	1.02	1.798	1.7m	980.348m	479.817m

Table S6. LSV results obtained in this research in comparison with other related studies in room temperature.

Electrocatalyst	Electrolyte	η_{10} (mV)	η_{100} (mV)	Tafel Slope (mV.dec^{-1})	Ref.
Co-Ni	1M KOH	132	-	84.39	[1]
Ni-Fe	1M KOH	142	239	133.3	[2]
Ni-Co	1M KOH	86.7	-	69.8	[3]
Ni-Cu	1M KOH	76	167	46	[4]
Mn-Co	1M KOH	100	-	65.4	[5]
Ni-Mg-La	1M KOH	70	-	120.26	[6]
Ni-Co-Mo	0.1M KOH	132	-	108	[7]
Co-Mo-Cu	6 M KOH	119	-	82	[8]
Ni-Cu-Fe	1M KOH	42	-	77	[9]
Ni-Co-Mn	1M KOH	81	214	118.73	This study

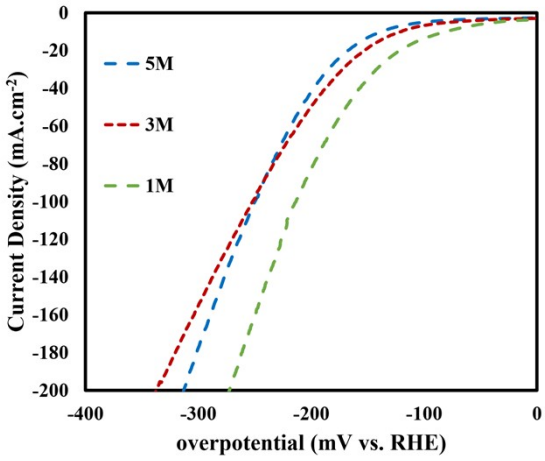

Figure S9. LSV curves of C3-S10 samples in different concentrations of KOH

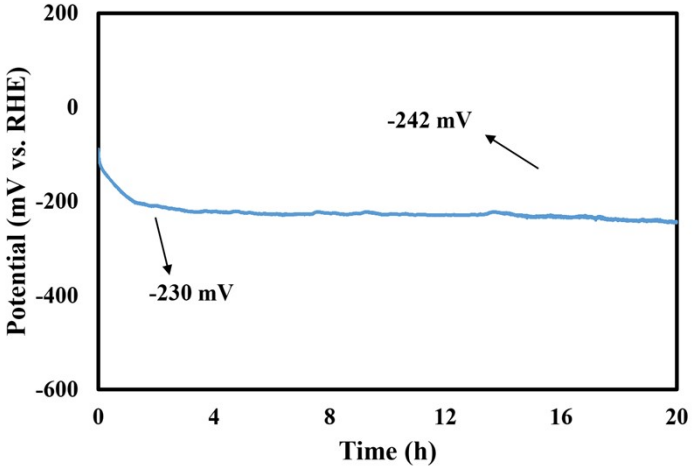

Figure S10. Long-term stability of C3-S10 in 5M KOH at 50 °c

References

[1] C. Cheng *et al.*, "High-efficiency bifunctional electrocatalyst based on 3D freestanding Cu foam in situ armored CoNi alloy nanosheet arrays for overall water splitting," *Journal of Power Sources,* vol. 427, pp. 184-193, 2019.

[2] Z. Zhang, Y. Wu, and D. Zhang, "Potentiostatic electrodeposition of cost-effective and efficient Ni–Fe electrocatalysts on Ni foam for the alkaline hydrogen evolution reaction," *International Journal of Hydrogen Energy,* vol. 47, no. 3, pp. 1425-1434, 2022.

[3] X. Zhang *et al.*, "3D hierarchical nanostructured Ni–Co alloy electrodes on porous nickel for hydrogen evolution reaction," *International Journal of Hydrogen Energy,* vol. 44, no. 57, pp. 29946-29955, 2019.

[4] J. Niu *et al.*, "Ultrarapid synthesis Ni-Cu bifunctional electrocatalyst by self-etching electrodeposition for high-performance water splitting reaction," *Applied Surface Science,* vol. 561, p. 150030, 2021.

[5] D. Cao *et al.*, "Amorphous Manganese–Cobalt Nanosheets as Efficient Catalysts for Hydrogen Evolution Reaction (HER)," *Catalysis Surveys from Asia,* vol. 25, no. 4, pp. 437-444, 2021.

[6] W. Liu, W. Tan, H. He, and Y. Yang, "Electrodeposition of self–supported Ni–Mg–La electrocatalyst on Ni foam for efficient hydrogen evolution reaction," *Electrochimica Acta,* vol. 411, p. 140058, 2022.

[7] D. Gao *et al.*, "Three-dimensional dendritic structures of NiCoMo as efficient electrocatalysts for the hydrogen evolution reaction," *ACS Applied Materials & Interfaces,* vol. 9, no. 27, pp. 22420-22431, 2017.

[8] H. L. S. Santos, P. G. Corradini, M. Medina, and L. H. Mascaro, "Effect of copper addition on cobalt-molybdenum electrodeposited coatings for the hydrogen evolution reaction in alkaline medium," *International Journal of Hydrogen Energy,* vol. 45, no. 58, pp. 33586-33597, 2020.

[9] Z. M. Kazemi, A. S. Rouhaghdam, G. B. Darband, M. Maleki, D. Han, and S. Shanmugam, "Ultra-fast electrochemical preparation of Ni-Cu-Fe nano-micro dendrite as a highly active and stable electrocatalyst for overall water splitting," *Electrochimica Acta,* vol. 456, p. 142468, 2023.